Interaction Between Typhoon Vicente (1208) and the Western Pacific Subtropical High During the Beijing Extreme Rainfall of 21 July 2012

WEN Yongren[1](文永仁), XUE Lin[2](薛 霖), LI Ying[2,3]*(李 英), WEI Na[2] (魏 娜), and LÜ Aimin[4] (吕爱民)

1 *Yunnan Meteorological Service Center, Kunming* 650034

2 *State Key Laboratory of Severe Weather, Chinese Academy of Meteorological Sciences, Beijing* 100081

3 *Shanghai Typhoon Institute, China Meteorological Administration, Shanghai* 200030

4 *National Meteorological Center, China Meteorological Administration, Beijing* 100081

(Received September 4, 2014; in final form December 2, 2014)

ABSTRACT

The heaviest rainfall in recent six decades fell in Beijing on 21 July 2012, reaching a record of 460 mm within 18 h. This rainfall was a typical remote precipitation event related to Typhoon Vicente (1208). Observational analysis indicates that Vicente influenced distant heavy rainfall by transporting water vapor northward to the Beijing area. This moisture transport was mainly driven by the interaction between Vicente and the western Pacific subtropical high (WPSH) associated with the formation of a low-level southeasterly moisture channel. A set of numerical sensitivity experiments were performed with prescribed typhoons of different intensities to investigate the interaction between Vicente and the WPSH and its effects on this rainstorm process. The results indicate that the WPSH interacting with typhoons of different intensities may exert varying degrees of influence on the development of a southeasterly moisture channel, resulting in a change in rain rate and location over the Beijing area. Specifically, in the presence of an enhanced typhoon, the WPSH shows remarkable withdrawal to the east, which is favorable for a northward extension of the southeasterly moisture channel, thereby increasing moisture supply for the rainstorm. The WPSH tends to stretch westward in a zonal pattern if the typhoon is weakened or removed, hindering the northward extension of the moisture channel. Thus, the rainfall area may be expected to expand or contract, with corresponding increases or decreases in rain rate over the Beijing area with a strengthened or weakened typhoon, respectively.

Key words: typhoon, remote precipitation, subtropical high, moisture transport

Citation: Wen Yongren, Xue Lin, Li Ying, et al., 2015: Interaction between Typhoon Vicente (1208) and the western Pacific subtropical high during the Beijing extreme rainfall of 21 July 2012. *J. Meteor. Res.*, **29**(2), 293–304, doi: 10.1007/s13351-015-4097-8.

1. Introduction

The heaviest rainfall in recent six decades fell in Beijing on 21 July 2012, reaching a record of 460 mm within 18 h, with the hourly rainfall rate exceeding 85 mm (Zhang et al., 2013). Sun et al. (2013) found that multiple synoptic systems influenced this extreme rainfall event, including a westerly trough, a cold front, a low-level mesoscale vortex, and moisture jet streams. Typhoon Vicente (1208) in the South China Sea was considered to provide favorable conditions for transporting moisture from the ocean to the rainfall area. Zhang et al. (2013) indicated that the progression of Typhoon Vicente from the South China Sea toward Guangdong Province altered the southwesterly monsoonal flow ahead of the cold front by weakening it in central China and reducing frontal rainfall.

Distant tropical cyclones (TCs) over the coastal regions of South China are usually found to be related to rainstorm events in North China (Jiang, 1983; Sun and Zhao, 2000; Ding et al., 2001; Cong et al., 2011, 2012), particularly from mid July to late August when

Supported by the National (Key) Basic Research and Development (973) Program of China (2015CB452804 and 2009CB421504) and National Natural Science Foundation of China (91215302, 41175063, 41275066, and 41475055).

*Corresponding author: liying@cams.cma.gov.cn.

TCs are active in the western North Pacific (WNP). Chen (2007) defined such rainfall, occurring outside the typhoon circulation but having a physical connection with the typhoon, as typhoon remote precipitation (TRP). Cong et al. (2011) investigated the statistical characteristics of TRP events in China from 1971 to 2006 and noted that, while TRP events occurred in 27 provinces across China, high frequencies were particularly observed in North China. Furthermore, Hou et al. (2006) showed that the correlation between extreme rainstorms in Shanxi Province in Northwest China and near-coast typhoons could reach 87%, and Sun et al. (2005) found that the TRP events in North China are closely linked to the interaction between westerly troughs and distant typhoons.

TRP events were also found in Japan and Korea. Wang et al. (2009) illustrated how Typhoon Songda (0418) enhanced precipitation over central Japan. It seems that the effect of southerly typhoons is to enhance northward moisture transport into a preconditioned precipitation region. Murata (2009) also demonstrated that the moisture supply associated with the outer circulation of a typhoon is a crucial factor for the enhancement of rainfall along the mountains in Kii Peninsula in Japan. Yoshida and Itoh (2012) found that Typhoon Maggie (9903) enhanced southerly moisture flux and caused the northward advection of a separate tropical disturbance, leading to heavy rainfall in the vicinity of Kyushu. Similarly, Byun and Lee (2012) identified the critical factors resulting in TRP events from a remote typhoon as a convectively unstable environment and large-scale convergence.

Similar distant effects from hurricanes in North Atlantic were first documented by Bosart and Carr (1978) in a case study on Hurricane Agnes (1972). A weak short-wavelength wave in the middle to upper troposphere triggered the growth of remote heavy rainfall, and the moisture channel associated with the circulation of Hurricane Agnes provided abundant water vapor from the western Atlantic to the rainfall area, significantly enhancing the rate and total amount of rainfall. Cote (2007) classified this type of TC rainfall, which occurs in advance of recurving TCs over the eastern United States, as a predecessor rain event (PRE). Schumacher et al. (2011) suggested that deep moisture originating from Hurricane Erin (2007) maximized low-level frontogenesis, thereby sustaining the mesoscale convective system in the rainfall region. Galarneau et al. (2010) and Bosart et al. (2012) also showed that the indirect effects of TCs include moisture transport in their outer circulation, which drives the growth of PREs.

It is evident from the previous studies described above that TCs exert a remarkable effect on distant precipitation, and the moisture transport associated with their outer circulation is a crucial factor in the enhancement of rainfall. However, the development of the moisture channel and its impacts on TRP are still not fully understood and require further detailed investigations. In the WNP, the western Pacific subtropical high (WPSH) plays an important role in the development of TCs, including the formation of moisture channels associated with TC circulation, that affects remote rainfall.

This study aims to explore the interactions between TCs and the WPSH, and to evaluate their combined impacts on TRP events through the case study of the extreme Beijing rainstorm of 21 July 2012. Various datasets, including the NCEP Global Forecast System's (GFS) global data ($0.5°\times0.5°$, 6 hourly, downloaded from http://rda.ucar.edu/datasets/ds335.0/index.html#sfolwl-/data/ds335.0?g=9), surface observation data, and typhoon best-track data from the China Meteorological Administration, are used in this study. Note: the GFS global data are a subset of the NCAR Historical Unidata Intenet Data Distribution (IDD) Gridded Model Data (ds335.0). The Advanced Research Weather Research and Forecasting (ARW-WRF) model is used to perform numerical simulations and sensitivity experiments. Section 2 describes the extreme rainfall event in Beijing on 21 July 2012 and its numerical simulations. Section 3 presents an analysis of the sensitivity experiment results. Finally, the conclusions are given in Section 4.

2. Numerical simulation of the Beijing rainstorm of 21 July 2012

2.1 Overview

Figure 1 shows the 500-hPa geopotential height distribution at 1200 UTC 21 July 2012, when the rainstorm occurred in the Beijing area (indicated by the pink closed loop). It is found that a westerly trough (brown line) was present to the north of China at this time. The WPSH body, indicated by the 5880-gpm geopotential height isoline, subsequently withdrew eastward and remained over the East China Sea, while Typhoon Vicente moved westward after passing through the Bashi Channel. At the same time, a low-level vortex (indicated by D in Figs. 1 and 2) at 850 hPa, originated in the northeast of the Qinghai-Tibetan Plateau, moved northeastward, and arrived in the Beijing area at 1200 UTC 21 July (blue line in Fig. 1). It developed with its central geopotential height decreased by 20 gpm in the subsequent 6 h, corresponding to a peak in the 1-h accumulated rainfall over Beijing (Fig. 3b). The rainstorm ceased after the vortex center left the Beijing area.

Additionally, two water vapor channels were connected to the Beijing area at 850 hPa during the rainfall event (Fig. 2). The first was a low-level southwesterly moisture jet from the Bay of Bengal, which transported water vapor to the north via the Indochina Peninsula and central China. This delivered a large moisture flux ($\geqslant 9\times10^{-3}$ g cm^{-1} h Pa^{-1} s^{-1}), which arrived in the Beijing area at 0000 UTC 21 July, before the rainstorm began (Fig. 2a). The second was a low-level southeasterly moisture jet extending between Vicente and the WPSH. This flow, with a large moisture flux, stretched northward and arrived in North China at 0600 UTC 21 July (Fig. 2b). The

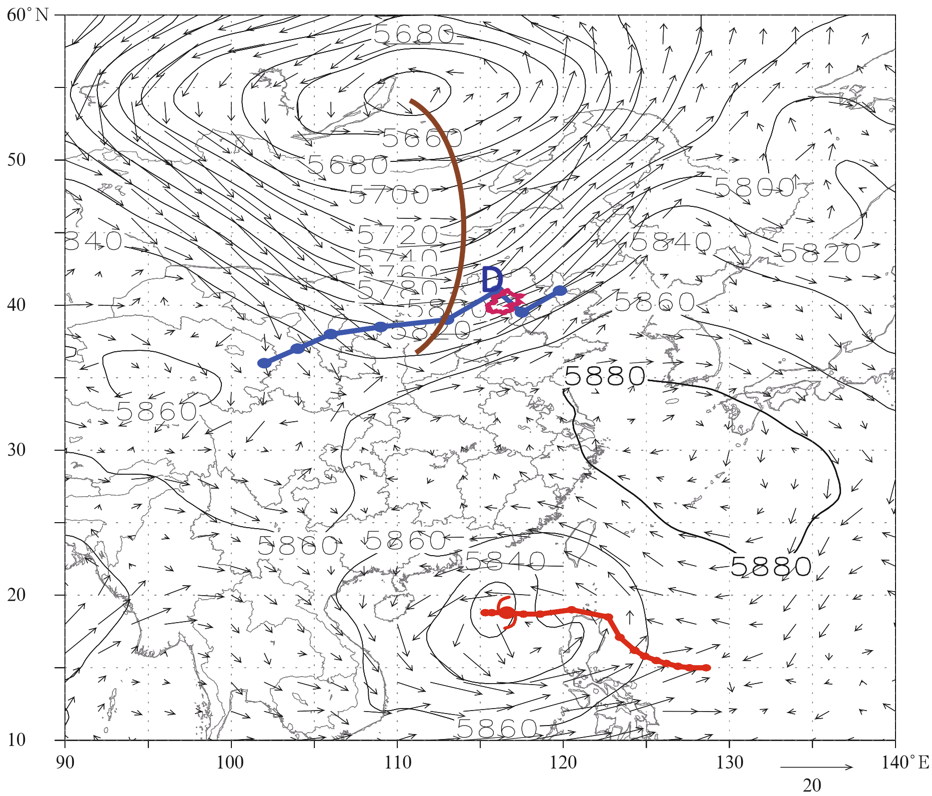

Fig. 1. Distribution of geopotential height (contours; gpm) and wind vectors (arrows; m s^{-1}) at 500 hPa at 1200 UTC 21 July 2012 from the GFS global data. The pink closed loop denotes the Beijing area; the typhoon symbol indicates Vicente's location at this time, the red line with dots shows its track between 1200 UTC 18 and 0000 UTC 22 July at 6-h intervals; the brown line indicates a westerly trough; the letter D shows the location of the low-level vortex, and the blue line indicates its track at 850 hPa at 6-h intervals.

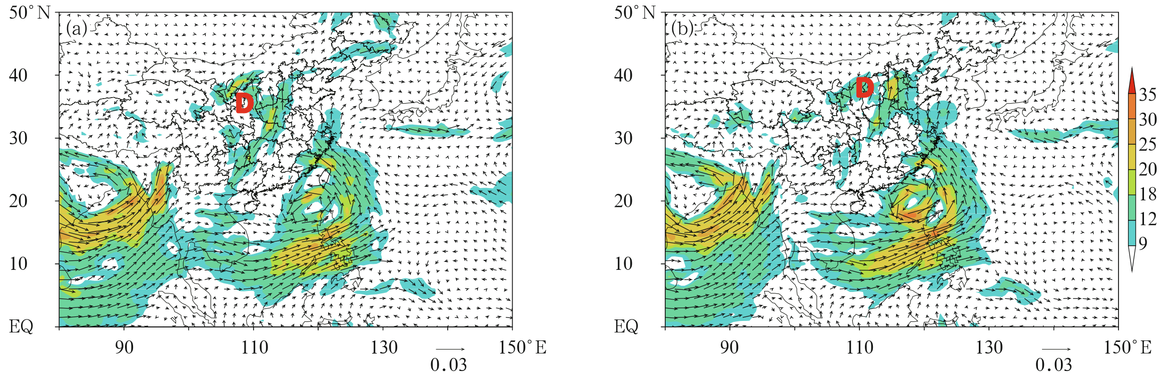

Fig. 2. Distributions of moisture flux vectors (10^{-3} g cm^{-1} hPa^{-1} s^{-1}; shadings indicate the regions with flux values $\geqslant 9\times10^{-3}$ g cm^{-1} hPa^{-1} s^{-1}) at 850 hPa at (a) 0000 UTC and (b) 0600 UTC 21 July from the GFS global data.

two moisture channels converged near the Beijing area and provided abundant water vapor for the rainfall event. During the rainfall process, the southwesterly channel was gradually weakened, but the southeasterly channel was enhanced, indicating its major role in supplying water vapor to the Beijing rainfall.

Generally, it may be concluded that the heavy rainfall in Beijing on 21 July 2012 was triggered by the interactions of the westerly trough, a low-level vortex from Northwest China, and moisture transport from the two low-level channels. The moisture jet between Vicente and the WPSH was found to play an important role in supplying water vapor for the heavy rainfall. To further investigate the formation of this moisture channel and its impact on the Beijing rainfall, a set of sensitivity experiments were performed with TCs of different intensities on the basis of the ARW-WRF model.

2.2 Model configuration and verification

The ARW-WRF model version 3.4 with two-way nested grids of 15- and 5-km horizontal spacings was employed in the following numerical simulations. The fine-grid domain primarily covered North China, the Huang-Huai area, and the Jiang-Huai area (see Fig. 5a). The following schemes were used for both domains: the Lin et al. microphysics scheme (Lin et al., 1983), the Mellor-Yamada-Janjic planetary boundary layer scheme (Janjic, 1994), the RRTM longwave radiation scheme (Mlawer et al., 1997), and the Dudhia shortwave radiation scheme (Dudhia, 1989). The Kain-Fritsch cumulus convection scheme (Kain, 2004) was used in domain 1 (D01; Fig. 5a) only. The NCEP GFS 0.5×0.5 global data were used to provide initial and lateral boundary conditions, which were updated

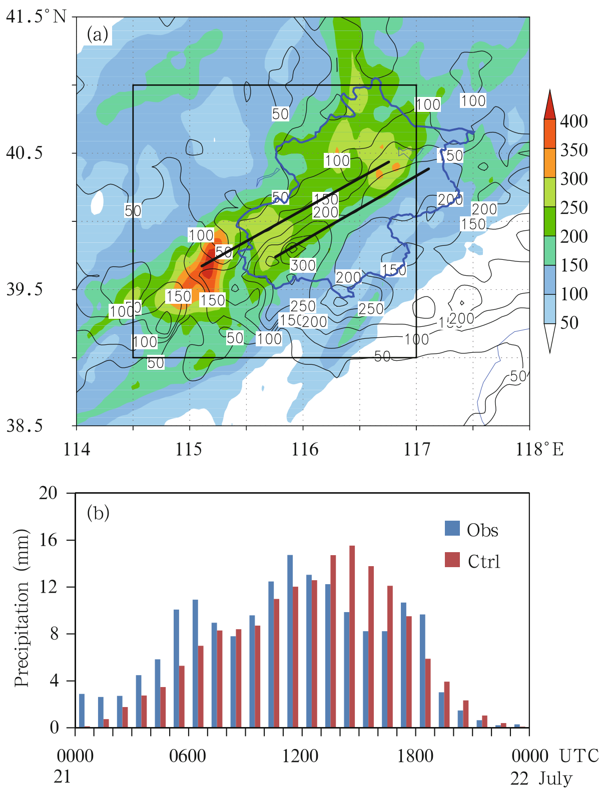

Fig. 3. (a) Distribution of observed (contours) and simulated (shaded) 24-h accumulated rainfall (mm) from 0000 UTC 21 to 0000 UTC 22 July 2012 (blue closed loop denotes the Beijing area; solid lines indicate the strike of rainbands). (b) Time series of observed (blue) and simulated (red) 1-h accumulated rainfall averaged over the heavy rainfall area denoted by the black box in (a).

every 6 h. The simulation ran from 1200 UTC 20 to 1200 UTC 22 July 2012, including the heavy rainfall process.

Figure 3a shows the distribution of simulated accumulative rainfall on 21 July compared with observed data. The simulated rainband occurred over the Beijing area and Hebei Province, stretching from southwest to northeast, as indicated by the black solid line, with several rainfall centers. This was similar to the observed rainband, except for a northwestward deviation in the position of around 0.3 latitude degree. The simulated maximum daily rainfall was 402 mm, occurring in the southwest part of the rainband, which was slightly less than the observed value of 460 mm. However, a second simulated rainfall center in the northeastern part of the rainband had a maximum daily rainfall of 300 mm, which was more than the nearby observations of approximately 200 mm.

Figure 3b compares the observed and simulated temporal variation in 1-h accumulated rainfall, averaged over the heavy rainfall area of 39°–41°N, 114.5°–117°E (the black box in Fig. 3a). The trends of observed and simulated rain rates are similar, with a peak around 1200 UTC 21 July, although the simulation shows a delay of approximately 3 h. The maximum rain rates from both observation and simulation around 15 mm h^{-1}. Thus, the simulation has quite reasonably described the rain rate and rainfall distribution over Beijing on 21 July 2012. This simulation is therefore used as a control run (Ctrl) to provide comparison for sensitivity experiments in the following text. Additionally, under these conditions, the westward track of Vicente was simulated with a little northward deviation (red and black lines denote the observed and simulated tracks respectively in Figs. 5a and 5b); however, its intensification process was predicted reasonably well (Fig. 5c).

2.3 Sensitivity experiments and results

Four sensitivity experiments were designed to investigate the impact of typhoons on rainfall over Beijing. The model configurations are the same as in the Ctrl simulation mentioned above, except for TC intensity. A spatial scale separation method provided by Lu and He (1992) was used to alter TC intensity. For this method, Legendre spherical harmonics are used to divide the meteorological elements into high and low frequency waves according to a cutoff wavenumber. Given that a TC is approximately 800 km in diameter, the cutoff wavenumber is set as 15, i.e., the TC circulation is dominated by high frequency waves. New circulation fields, including TC circulations of different intensities, are built through a modification of the high frequency waves, which can be expressed as follows:

$$H = H_\mathrm{l} + s \times H_\mathrm{h},$$

where H represents an atmospheric physical element, H_l is the low frequency wave, H_h is the high frequency wave, and s is defined as a weight coefficient. In this case, H_h was modified within the TC area of 13°–24°N, 111°–129°E in the initial fields. If $s < 1.0$ or $s > 1.0$, the TC would be weakened or strengthened, and if $s = 1.0$, the TC would retain its original intensity. This method has been used successfully for westerly trough modifications in previous studies by Meng et al. (2002) and Li et al. (2006).

In our sensitivity experiments, s is set as 0.0, 0.5, 1.5, and 2.0 for experiments W1, W2, S1, and S2, respectively, to change the wind components u and v, and geopotential height of the initial fields. Considering the potential effects of the lateral boundary conditions during the integral process, the GFS global data used to form lateral boundary conditions were also modified in the same way. Figure 4 shows the initial fields at 1200 UTC 20 July 2012 when Vicente had just formed in the five different simulations. Compared with the Ctrl (Fig. 4a), the TC disturbance was removed in W1 (Fig. 4b) and was weakened in W2 (Fig. 4c). In both S1 (Fig. 4d) and S2 (Fig. 4e), TC circulations were stronger than in the Ctrl, and this was particularly more prominent in S2.

Figure 5 displays the tracks and changes in intensity of the TCs in all simulations during the integration period. TC tracks in the sensitivity experiments were similar to that in the Ctrl, with a maximum error of approximately 170 km in the later periods (Fig. 5b). TC intensity also changed over time reasonably consistently (Fig. 5c). In general, TCs were enhanced in S1 and S2 and diminished in W2 and W1 compared with the Ctrl during the integration period, implying that the intensity of the TCs was effectively modified according to the design requirements of the sensitivity experiments. In W1, entire TC circulation was removed at the initial time and the low depression occurring subsequently was too weak to be defined as a typhoon.

Figure 6 compares the distributions of heavy daily

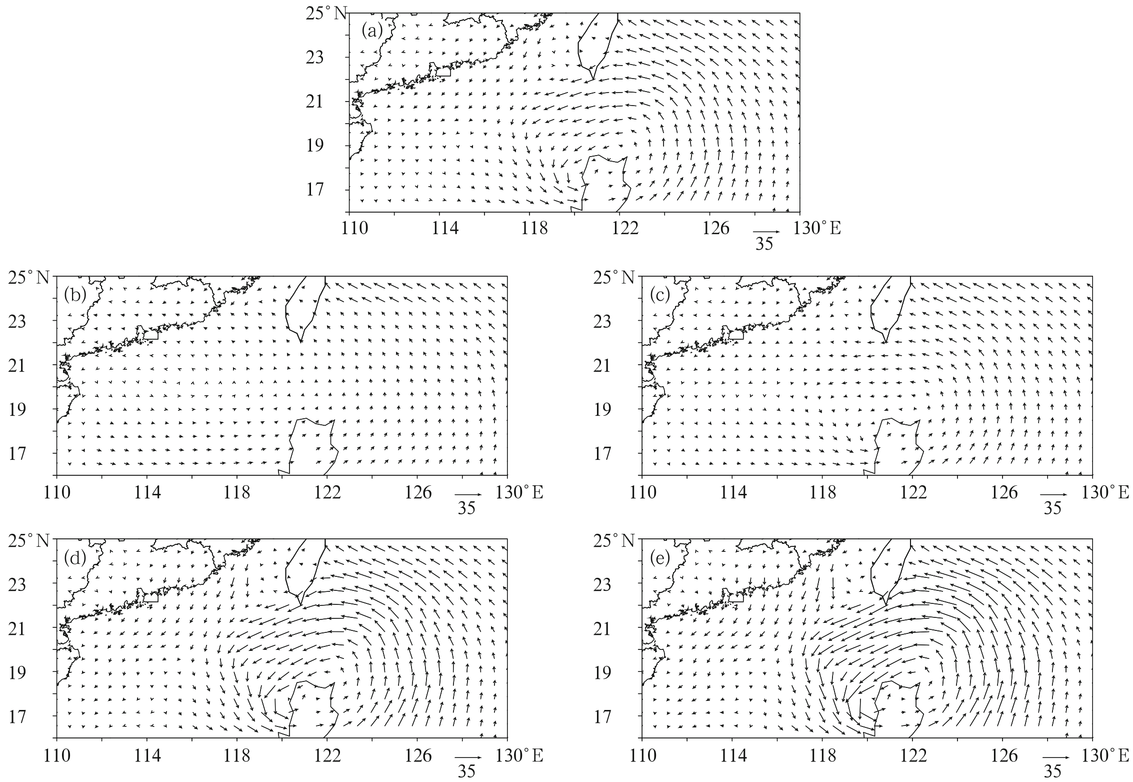

Fig. 4. Initial wind vectors (m s^{-1}) at 1200 UTC 20 July 2012 for (a) Ctrl, (b) W1, (c) W2, (d) S1, and (e) S2.

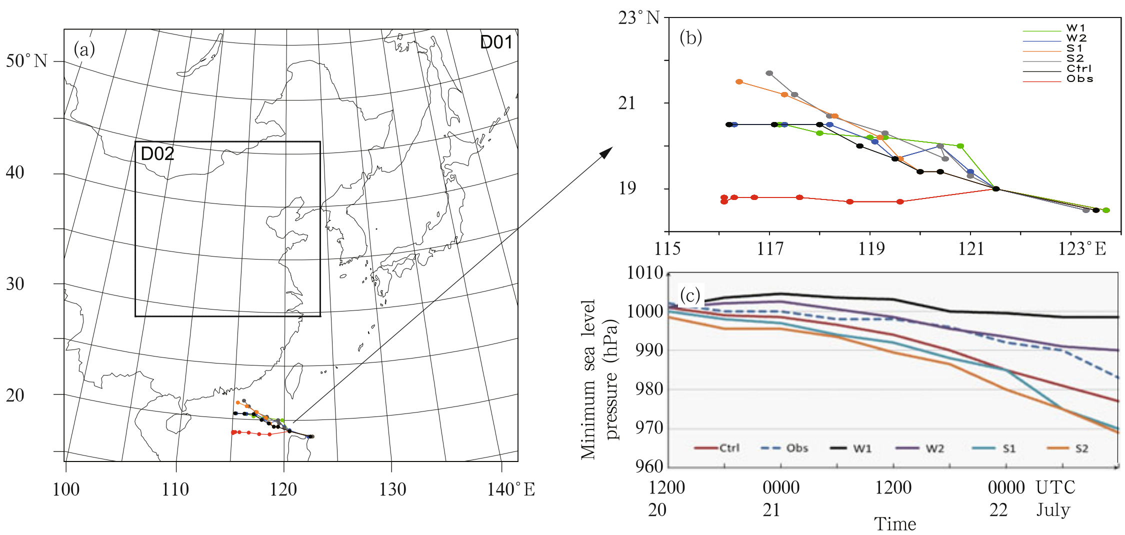

Fig. 5. (a) Simulation domains (the rectangle labeled D02 denotes the fine-grid area) with observed and simulated TC tracks, (b) typhoon tracks on a smaller scale, and (c) time series of the minimum sea level pressure (hPa) at the typhoon center during the integration period.

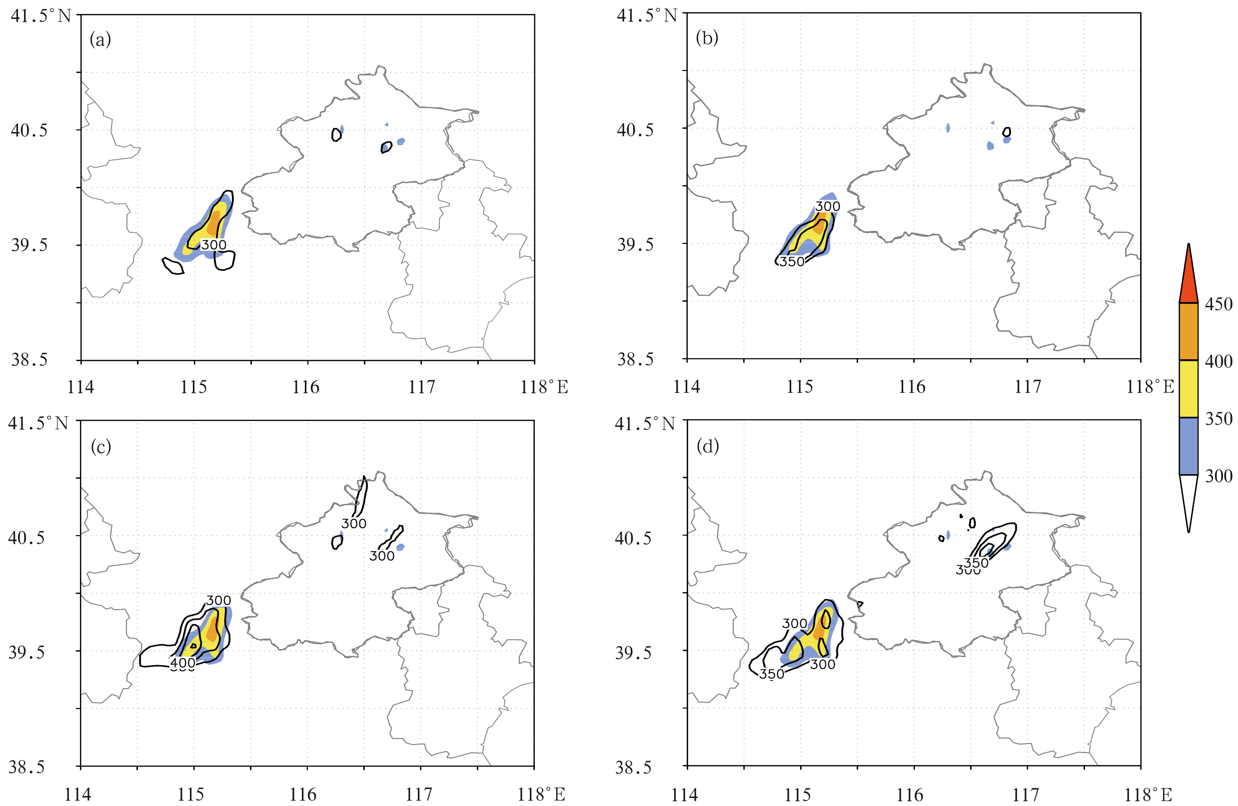

Fig. 6. 24-h accumulated rainfall (mm) distributions (exceeding 300 mm only) in the Ctrl (shaded) and sensitivity (contours) experiments on 21 July 2012 for experiments (a) W1, (b) W2, (c) S1, and (d) S2.

rainfall (greater than 300 mm only) in the Ctrl (shaded) and sensitivity experiments (contours) on 21 July. In W1 (Fig. 6a), the rain rate showed a distinct decrease, with a maximum reduction of 90 mm at the southwest rainfall center, while the heavy rainfall area generally contracted and dispersed. In W2 (Fig. 6b), the maximum rain rate decreased by 60 mm, and the heavy rainfall area also contracted slightly. In both stronger typhoon runs, S1 and S2 (Figs. 6c and 6d), the areas of heavy rainfall were expanded, particularly in the northeast parts of the rainband. The maximum rain rate was observed to increase significantly at both rainfall centers in S1. For S2, the maximum rain rate at the southwest rainfall center was slightly less than the Ctrl, but was doubled in the northeast rainfall center. Thus, an enhanced (weakened) TC could be expected to extend (contract) the rainfall area northward and increase (reduce) the rain rate. The two simulations with the most notable differences, W1 and S2, are particularly focused on in the following sections.

3. Further analysis

3.1 Atmospheric circulation

A TC over the WNP usually moves along the southern edge of the WPSH, interacting with the WPSH along its track (Chen and Ding, 1979). Figure 7 shows the variation in the WPSH represented by the 5880-gpm geopotential height isolines (solid lines) in all simulations. The WPSH was connected with the continental high over South China in all experiments at 0000 UTC 21 July before the Beijing rainstorm began (Fig. 7a). These two highs would subsequently break over South China. At 1800 UTC 21 (Fig. 7c), the 5880-gpm isoline was broken and the WPSH retreated eastward quite obviously in S2 (blue line), and the WPSH disconnected from the continental high and withdrew somewhat eastward in S1 and Ctrl (orange and red lines, respectively); however, the two highs remained connected in W1 and W2 (black and green lines, re-

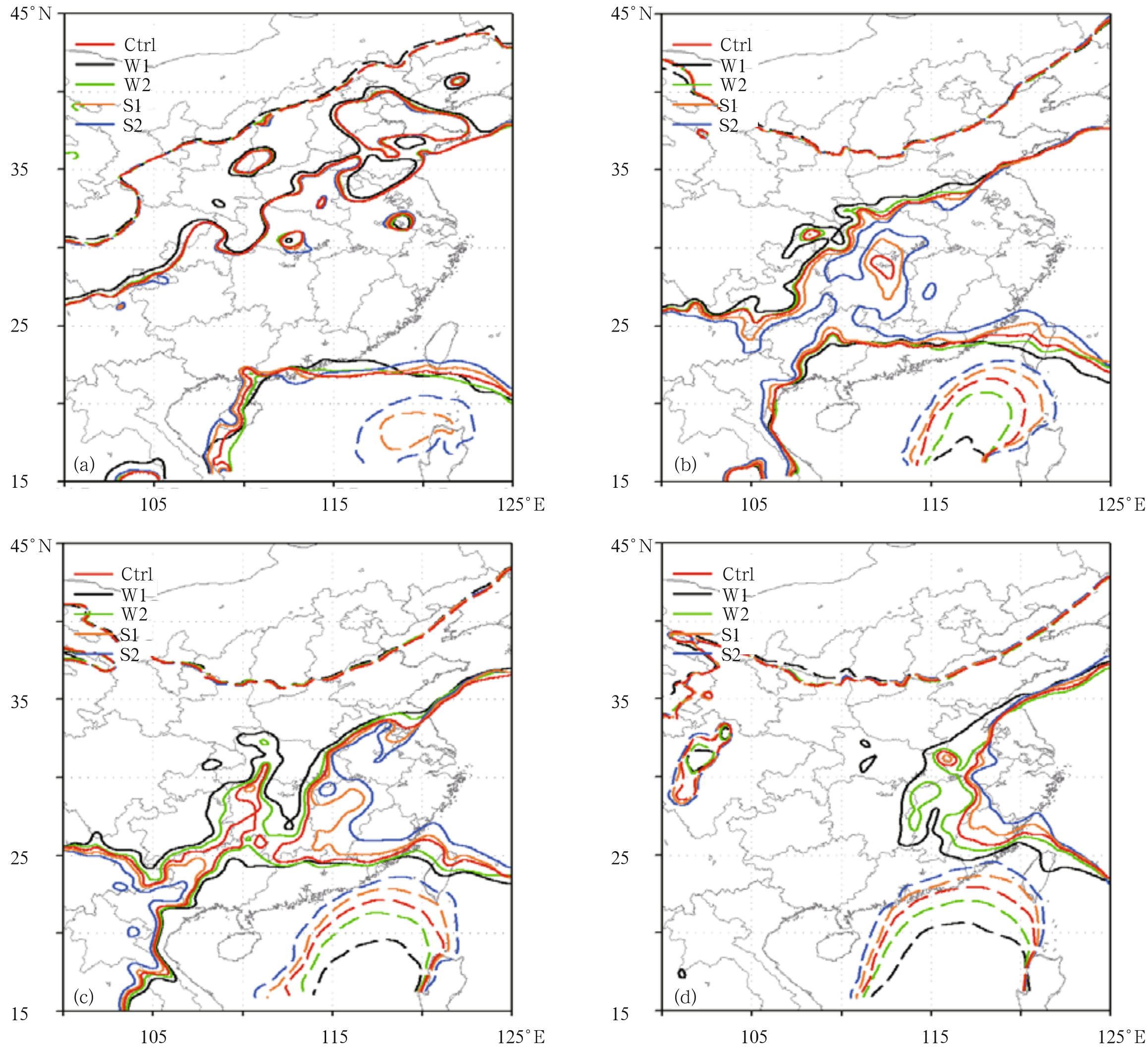

Fig. 7. Comparison of distributions of 5880- (solid lines) and 5840-gpm (dashed lines) geopotential height isolines between the five simulations at (a) 0000 UTC 21, (b) 1500 UTC 21, (c) 1800 UTC 21, and (d) 0000 UTC 22 July.

spectively, in Fig. 7c) until 2100 UTC 21 July (figures omitted). Because of the difference in timing of the WPSH disconnection from the continental high and its subsequent eastward movement, the positions of the WPSH's western edge in the four experiments are different. In particular, the WPSH in S2 was approximately 4° in longitude further east than in W1 by 0000 UTC 22 July (Fig. 7d). Thus, it can be inferred that a strengthened TC is more favorable to the eastward withdrawal of the WPSH. A stronger TC is usually associated with stronger horizontal vorticity and stronger cyclonic wind circulation (see the dashed isolines over the South China Sea in Fig. 7d, see also Fig. 4). When moving northward, the stronger TC usually results in greater positive vorticity-driven convection, together with the larger-scale cyclonic circulation, pushing the WPSH to retreat eastward. Notably, there was little difference in the positions of the 5840-gpm isolines (dashed lines) over the midlatitude areas among the sensitivity experiments, indicating that the position of the westerly trough was barely affected by changes in the distant TCs.

3.2 Moisture transport

As shown in Fig. 8a, the moisture transport channels for the Beijing rainstorm comprise a low-level southwesterly jet over the mainland of China, and a low-level southeasterly jet between the TC and the

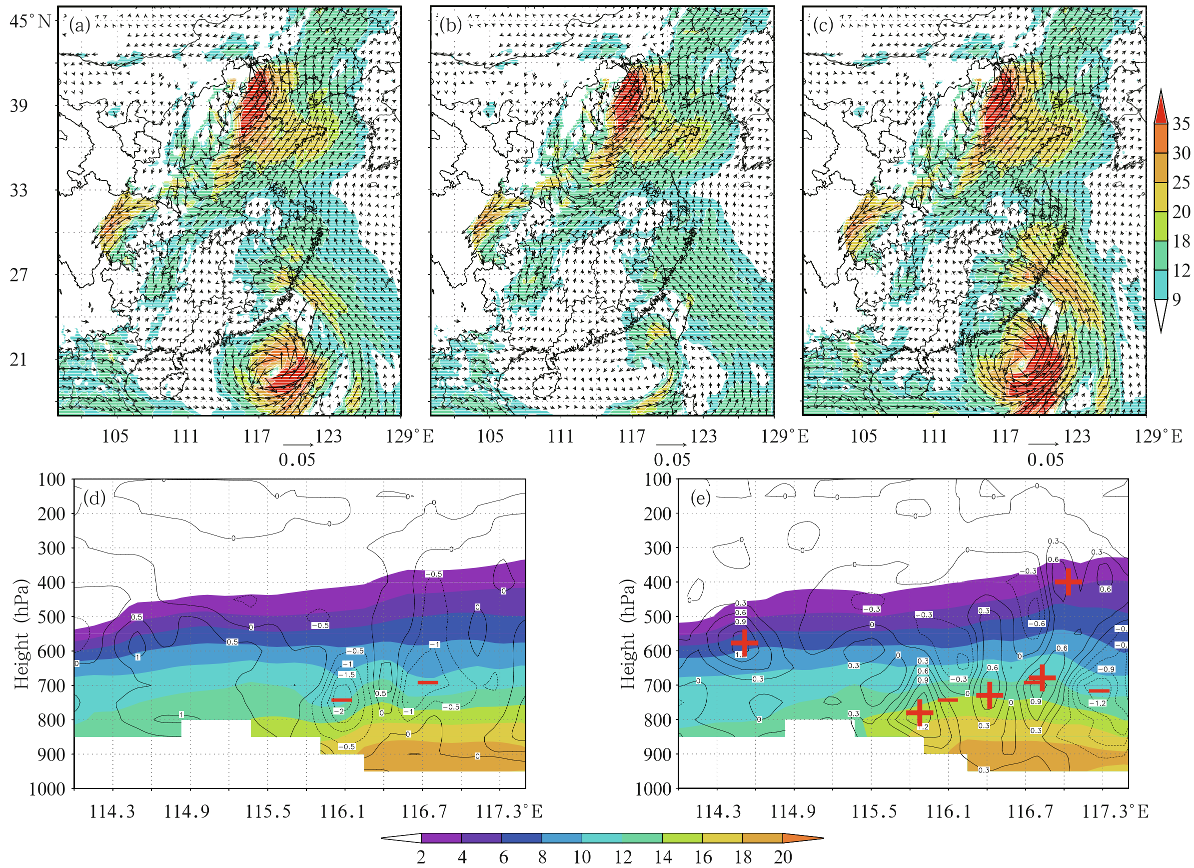

Fig. 8. Distributions of water vapor flux vectors (10^{-3} g cm^{-1} hPa^{-1} s^{-1}; shaded area indicates values of $\geqslant 9\times10^{-3}$ g cm^{-1} hPa^{-1} s^{-1}) at 850 hPa in (a) Ctrl, (b) W1, and (c) S2; and vertical distributions of specific humidity (shaded; g kg^{-1}) and their difference with the Ctrl (contours; g kg^{-1}) along 40°N at 1800 UTC 21 July in (d) W1 and (e) S2. The symbols "–" and "+" indicate negative and positive anomaly centers of specific humidity, respectively.

WPSH, which are similar to the GFS global data (Fig. 2). It can be seen that the southwesterly channel varied slightly between the Ctrl and sensitivity experiments, in either intensity or location. However, the southeasterly jet showed remarkable differences corresponding to changes in the TC intensity. Compared with the values in Ctrl, the maximum water vapor flux in the TC's northeastern envelope increased to 30 $\times$ 10^{-3} g cm^{-1} hPa^{-1} s^{-1} in S2 (Fig. 8c), but decreased to 18 $\times$ 10^{-3} g cm^{-1} hPa^{-1} s^{-1} in W1 (Fig. 8b). Additionally, the moisture plume associated with the TC in S2 was approximately 6° in latitude further north than that in W1, indicating that a stronger TC is favorable for the transport of water vapor to a remote rainfall area in the north. Such transport is attributed to the interaction between the TC and the WPSH. The WPSH would withdraw further eastward, and do so earlier, if it interacted with a stronger TC, allowing more water vapor to reach higher latitudes via the channel between the WPSH and TC. In the absence of a strong TC, the WPSH would retreat eastward later and maintain a west-east zonal shape for a longer time, thereby blocking northward water vapor transport from the ocean in the south.

Figures 8d and 8e show vertical cross-sections of specific humidity along 40°N in W1 and S2 and their differences compared with the Ctrl at 1800 UTC 21 July. The most remarkable difference occurred between 115°25′ and 117°35′E, which represents the rainfall area over Beijing in both simulations. A maximum decrease center ($\leqslant -2$ g kg^{-1}) and a second center ($\leqslant -1$ g kg^{-1}) could be found near 700 hPa in W1 (Fig. 8d), while a series of positive abnormal centers, denoted by "+" in

Fig. 8e, could be found over the Beijing area in S2 (Fig. 8e). Therefore, the high moisture layer was notably deeper in S2 than that in W1, indicating that a stronger TC would increase the magnitude of water vapor supply for the heavy rainfall.

3.3 Local precipitation conditions

As mentioned in Section 3.2, TCs of different intensities would impact the activity of the WPSH and low-level moisture transport, which may alter the local precipitation conditions of remote rainy areas in turn. Comparison of the time series of vertical velocity near the heavy rainfall center (40.5°N, 116.7°E) in the northeastern part of the rainband shows salient differences between W1 and S2 during the rainstorm (Figs. 9a–c). Compared with the Ctrl (Fig. 9a), the updrafts decreased substantially in W1 (Fig. 9b), but significantly increased in S2 (Fig. 9c), with the largest increase of approximately 70 × 10^{-2} m s^{-1}. This suggests that local upward motion over the rainfall area is also sensitive to remote TC intensity. Moreover, the strongest ascending motion was found mainly in the high-level troposphere in S2, implying the development of deeper convection in the presence of an enhanced TC.

Figures 9d–f show the temporal evolution of the vorticity (contours) and divergence (shading) over the heavy rainfall center (40.5°N, 116.7°E). During the

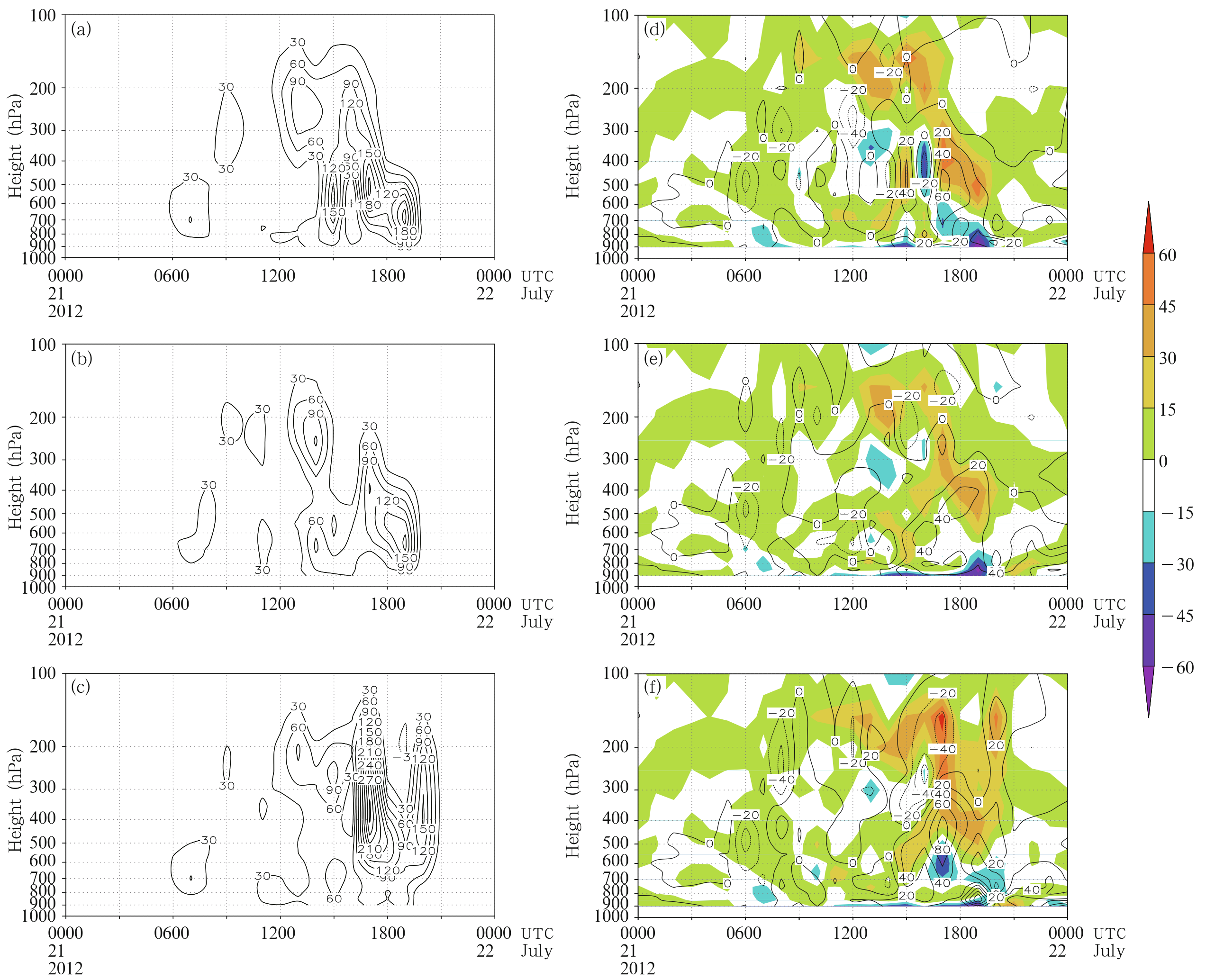

Fig. 9. Temporal variations of vertical velocity (10^{-2} m s^{-1}) in (a) Ctrl, (b) W1, and (c) S2, and temporal evolution of vorticity (contours; 10^{-5}s^{-1}) and divergence (shading; 10^{-5} s^{-1}) in (d) Ctrl, (e) W1, and (f) S2 at the heavy rainfall center (40.5°N, 116.7°E).

heavy rainfall period from 1500 to 2100 UTC 21 July, positive vorticity and negative divergence were observed in the lower troposphere, whereas negative vorticity and positive divergence were dominant in the upper troposphere for all three simulations. This is characterized by cyclonic convergence in the lower layer and anticyclonic divergence in the upper layers. However, positive vorticity in the middle and lower layers decreased notably when the TC was removed in W1 (Fig. 9e) compared with the Ctrl (Fig. 9d). In contrast, both positive vorticity in the lower layers and negative vorticity in the upper layers were strengthened in S2 (Fig. 9f), implying that deeper convection occurred in the rainfall area under an enhanced TC. Thus, we can conclude that the local weather conditions in Beijing become more favorable for a rainstorm under the effects of a stronger remote TC.

The variations in local rainfall conditions are closely related to the combined effects of TCs and the WPSH. In strengthened TC experiments (e.g., S2), a strong southeasterly moisture channel developed and water vapor was easily transported from the tropical ocean to the low-level vortex area around Beijing (see Fig. 2). Consequently, the vorticity in the lower layer was enhanced, which contributed to the development of a high-level southwesterly jet stream ahead of the westerly trough. This in turn resulted in the intensification of the high-level divergence on its right side over the Beijing area. However, in the experiments with a weakened or removed TC (e.g., W1), the moisture channel was also weakened and water vapor transport to the north was blocked by the WPSH, which is generally unfavorable for the development of a vortex in the Beijing area.

4. Concluding remarks

The extreme rainfall event in Beijing on 21 July 2012 is closely related to the distant Typhoon Vicente through its supply of abundant water vapor to the northern rainy region. It has been shown that the moisture channel between Vicente and the WPSH played a key role in the rainstorm process. The interaction between the WPSH and the TC, and their associated impacts on the rainstorm were investigated based on a WRFV3.4 control simulation and four sensitivity experiments. The results indicate that TCs of different intensities can alter the rain rate and rainfall distribution in distant areas. The rain rate would be increased and the rain area would be expanded in the presence of a strengthened TC, and vice versa. These differences are mainly attributed to the interaction between TC and the WPSH. In the presence of an enhanced TC on its southwest side, the WPSH would withdraw earlier and further to the east, while the WPSH would retreat eastward later if the TC were removed or weakened. Thus, a strengthened TC would lead to enhancement of the low-level southeasterly moisture channel between the TC and the WPSH, allowing water vapor to be transported more northward along the rim of the WPSH. Conversely, the moisture channel would be weakened or blocked by the WPSH if the TC was weakened or removed.

It should be noted that the WPSH activity is dominant and can be affected by multiscale systems, such as a westerly trough, a Tibetan high, or a TC. To some extent, the impact of a TC on the WPSH may be minor, and limited by its circulation size and intensity. Therefore, the interaction between TCs and the WPSH may differ from case to case, and the general patterns found here should be verified further with more specific cases.

REFERENCES

Bosart, L. F., and F. H. Carr, 1978: A case study of excessive rainfall centered around Wellsville, New York. *Mon. Wea. Rev.*, **106**, 348–362.

Bosart, L. F., J. M. Cordeira, T. J. Galarneau, et al., 2012: An analysis of multiple predecessor rain events ahead of tropical cyclones Ike and Lowell: 10–15 September 2008. *Mon. Wea. Rev.*, **140**, 1081–1107.

Byun, K. Y., and T. Y. Lee, 2012: Remote effects of tropical cyclones on heavy rainfall over the Korean Peninsula—Statistical and composite analysis. *Tellus A*, **64**, 14983, doi: 10.3402/tellusa.v64i0.14983.

Chen Lianshou and Ding Yihui, 1979: *An Introduction to the Western Pacific Typhoon*. Science Press, Beijing, 491 pp. (in Chinese)

Chen Lianshou, 2007: The studies and predictions of heavy rainfall related to the landing tropical cyclones. The Abstracts of Papers on the Fourteenth Symposium on the Tropical Cyclones, Shanghai, China, 6–8 November, 3–7. (in Chinese)

Cong Chunhua, Chen Lianshou, Lei Xiaotu, et al., 2011: An overview on the study of tropical cyclone remote rainfall. *J. Trop. Meteor.*, **27**, 264–270. (in Chinese)

Cong Chunhua, Chen Lianshou, Lei Xiaotu, et al., 2012: A study on the mechanism of the tropical cyclone remote precipitation. *Acta Meteor. Sinica*, **70**, 717–727. (in Chinese)

Cote, M. R., 2007: Predecessor rain events in advance of tropical cyclones. Master dissertation, Department of Atmospheric and Environmental Sciences, University at Albany, State University of New York, 200 pp.

Ding Zhiying, Zhang Xinqiang, He Jinhai, et al., 2001: The study of storm rainfall caused by interaction between the non-zonal high level jet streak and the far distant typhoon. *J. Trop. Meteor.*, **17**, 144–154. (in Chinese)

Dudhia, J., 1989: Numerical study of convection observed during the winter monsoon experiment using a mesoscale two-dimensional model. *J. Atmos. Sci.*, **46**, 3077–3107.

Galarneau, T. J., L. F. Bosart, and R. S. Schumacher, 2010: Predecessor rain events ahead of tropical cyclones. *Mon. Wea. Rev.*, **138**, 3272–3297.

Hou Jianzhong, Zhang Hong, Du Jiwen, et al., 2006: Ambient field and cloud-picture characteristics of typhoon and cold-front heavy rainfall in northeastern Tibet. *Meteor. Sci. Technol.*, **34**, 41–46. (in Chinese)

Janjić, I. Zaviša, 1994: The step-mountain Eta coordinate model: Further developments of the convection, viscous sublayer, and turbulence closure schemes. *Mon. Wea. Rev.*, **122**, 927–945.

Jiang Shangcheng, 1983: A synoptic model of the hard rain storm in westerly belt affected by the far distant typhoon. *Acta Meteor. Sinica*, **41**, 147–158. (in Chinese)

Kain, J. S., 2004: The Kain-Fritsch convective parameterization: An update. *J. Appl. Meteor.*, **43**, 170–181.

Li Ying, Chen Lianshou, and Lei Xiaotu, 2006: Numerical study on impacts of upper-level westerly trough on the extratropical transition process of Typhoon Winnie (1997). *Acta Meteor. Sinica*, **64**, 552–563. (in Chinese)

Lin, Yuh-Lang, Richard D. Farley, and Harold D. Orville, 1983: Bulk parameterization of the snow field in a cloud model. *J. Climate Appl. Meteor.*, **22**, 1065–1092.

Lu Xianchi and He Bin, 1992: Two ways to perform initial data grid-spectral transform. *Chinese J. Comput. Physics.*, **9**, 768–770. (in Chinese)

Meng Zhiyong, Xu Xiangde, and Chen Lianshou, 2002: Mesoscale characteristics of the interaction between TC Tim (9406) and midlatitude circulation. *Acta Meteor. Sinica*, **60**, 31–39. (in Chinese)

Mlawer, E. J., S. J. Taubman, P. D. Brown, et al., 1997: Radiative transfer for inhomogeneous atmospheres: RRTM, a validated correlated-k model for the longwave. *J. Geophys. Res.*, **102**, 16663–16682.

Murata, A., 2009: A mechanism for heavy precipitation over the Kii Peninsula acompanying Typhoon Meari (2004). *J. Meteor. Soc. Japan*, **87**, 101–117.

Schumacher, R. S., T. J. Galarneau, and L. F. Bosart, 2011: Distant effects of a recurving tropical cyclone on rainfall in a midlatitude convective system: A high-impact predecessor rain event. *Mon. Wea. Rev.*, **139**, 650–667.

Sun Jianhua and Zhao Sixiong, 2000: Diagnoses and simulation of typhoon (Tim) landing and producing heavy rainfall in China. *Chinese J. Atmos. Sci.*, **24**, 223–237. (in Chinese)

Sun Jianhua, Zhang Xiaoling, Wei Jie, et al., 2005: A study on severe heavy rainfall in North China during the 1990s. *Climatic Environ. Res.*, **10**, 492–505. (in Chinese)

Sun Jianhua, Zhao Sixiong, Fu Shenming, et al., 2013: Multi-scale characteristics of record heavy rainfall over Beijing area on July 21, 2012. *Chinese J. Atmos. Sci.*, **37**, 705–718. (in Chinese)

Wang, Y. Q., Y. Q. Wang, and H. Fudeyasu, 2009: The role of Typhoon Songda (2004) in producing distantly located heavy rainfall in Japan. *Mon. Wea. Rev.*, **137**, 3699–3716.

Yoshida, K., and H. Itoh, 2012: Indirect effects of tropical cyclones on heavy rainfall events in Kyushu, Japan, during the Baiu season. *J. Meteor. Soc. Japan*, **90**, 377–401.

Zhang Dalin, Lin Yonghui, Zhao Ping, et al., 2013: The Beijing extreme rainfall of 21 July 2012: "Right results" but for wrong reasons. *Geophys. Res. Lett.*, **40**, 1426–1431.